Note: This copy is for your personal, non-commercial use only. To order presentation-ready copies for distribution to your colleagues or clients, contact us at www.rsna.org/rsnarights.





# T2 Mapping in Duchenne Muscular Dystrophy: Distribution of Disease Activity and Correlation with Clinical Assessments[1]

Hee Kyung Kim, MD
Tal Laor, MD
Paul S. Horn, PhD
Judy M. Racadio, MD
Brenda Wong, MD
Bernard J. Dardzinski, PhD[2]

**Purpose:** To analyze T2 maps of pelvic and thigh muscles in Duchenne muscular dystrophy (DMD), to identify the most severely affected muscle, and to correlate the T2 of muscle with the grade of fatty infiltration at nonquantitative magnetic resonance (MR) imaging and results of clinical assessment.

**Materials and Methods:** This prospective study was HIPAA compliant and was approved by the institutional review board; written consent was obtained from all participants' parents or guardians. Thirty-four boys with DMD (mean age, 8.4 years) were evaluated clinically (age, clinical function score, timed Gower score, time to run 30 feet, and serum creatine kinase [CK] level) and with nonquantitative MR imaging and axial T2 mapping from the iliac crest to the mid thigh. The T2 maps and mean T2 of 18 muscles in the pelvis and thighs were analyzed to identify the most severely involved muscle. The amount of fatty infiltration was assigned a grade of zero to four for all pelvic and thigh muscles by using T1-weighted nonquantitative MR images. The Spearman correlation coefficients model was used to correlate the mean T2, nonquantitative MR imaging score and clinical assessments.

**Results:** The gluteus maximus muscle had the highest T2. The mean T2 for this muscle showed a significant correlation with the nonquantitative MR imaging score for fatty infiltration ($P < .001$) and with all clinical assessments except CK level.

**Conclusion:** Gluteus maximus muscles are most severely affected in patients with DMD. The T2 of the gluteus maximus muscle can be used as a quantitative and objective measure of disease severity.

© RSNA, 2010

[1] From the Department of Radiology (H.K.K., T.L., J.M.R.), Department of Neurology (B.W.), and Imaging Research Center (B.J.D.), Cincinnati Children's Hospital Medical Center, 3333 Burnet Ave, Cincinnati, OH 45229-3039; and Department of Mathematical Sciences, University of Cincinnati, Cincinnati, Ohio (P.S.H.). Received August 21, 2009; revision requested September 23; final revision received November 20; accepted December 15; final version accepted January 11, 2010. **Address correspondence to** T.L. (e-mail: *laor@cchmc.org*).
[2] **Current address:** Merck Research Laboratories, West Point, Pa.

© RSNA, 2010

Duchenne muscular dystrophy (DMD) is one of the most common neuromuscular disorders in children (1). It is a fatal X-linked recessive muscular dystrophy with an overall incidence of one in 3500 boys (1). DMD is characterized by mutation or absence of dystrophin, which normally forms a membrane-bound glycoprotein complex in muscle tissue that helps maintain plasma membrane integrity (2). The absence of dystrophin in the muscle causes instability of plasma membranes and makes the muscle fragile and susceptible to injury during concentric contraction (3). Muscle injury, repair, and inflammatory changes are seen very early in the disease process and are then followed by fatty infiltration, which is irreversible (3,4).

DMD is characterized clinically by progressive muscle weakness, which starts in the proximal pelvic girdle and progresses distally into the extremities. Disease progression ultimately results in death, often during the 3rd decade (1). Early corticosteroid therapy can slow the progression of the muscle weakness by ameliorating the inflammatory process, but it cannot cure the disease (5). Furthermore, long-term treatment with high-dose corticosteroids is limited owing to the side effects, which include loss of bone mineralization and cataract formation (6). Gene therapy and myoblast transfer therapy are being evaluated as more specific ways of treating the pathologic process in DMD (7–9).

A clinical functional score (CFS) system, although developed to assess muscle strength in patients with DMD (10), has limitations—particularly in an uncooperative child. In addition, the CFS does not evaluate individual muscles (11,12). The level of serum creatine kinase (CK), a biochemical marker frequently obtained in these patients, also is not a reliable determinant of disease activity (13). Muscle biopsy has been used to establish the diagnosis of DMD and to evaluate the histologic changes in the muscle after treatment. Information obtained from muscle biopsy is limited to the site of sampling, not the entire muscle, and repeated muscle biopsy is impractical, especially in children. Therefore, it is important to have a noninvasive way to quantify the disease state so that the disease status and response to treatment can be monitored.

Nonquantitative magnetic resonance (MR) imaging has been used to characterize the pattern of fatty infiltration in DMD (14–16). With use of nonquantitative MR imaging, a relative selective sparing of fatty infiltration of the gracilis, sartorius, and semitendinosus muscles has been noted. Compositional analysis of muscles in boys with DMD showed that fatty infiltration was most prominent in the gluteus and adductor magnus muscles, whereas the quadriceps, adductor, and biceps femoris muscles were the muscles most affected by inflammation or edema (14–16). A correlation between the fatty infiltration grade at MR imaging and clinical assessments has also been demonstrated (15). However, evaluation of nonquantitative MR imaging findings of the fatty infiltration on T1-weighted images is a subjective method to assess disease severity.

T2 mapping has been previously performed at the level of the calf (hereafter called the lower leg) in patients with DMD. The T2 in those patients was found to be significantly increased compared with that of control subjects ($P < .05$). The increased T2 in patients with DMD is thought to result from fatty infiltration of the muscles because T2 is longer in fat than in muscle (17,18). Researchers in another study (19) in which T2 mapping of the muscles of the lower extremities was used in patients with dermatomyositis, another muscle disorder, showed an increased T2, which was thought to reflect inflammation. Therefore, T2 mapping may be an objective, quantitative method to monitor disease activity.

Although the disease process in DMD begins in the pelvic girdle and progresses distally, to our knowledge, T2 mapping has not yet been used to document disease distribution of the pelvic girdle. There also have been no studies to assess the correlation between T2 and clinical assessment of disease activity.

Therefore, the purpose of our study was to analyze T2 maps of individual pelvic and thigh muscles to try to define a characteristic disease distribution in DMD and to identify the most severely involved muscles. We also aimed to evaluate the T2 as a means of objectively measuring DMD disease activity by comparing the T2 map of the most severely affected muscle with subjective grading of fatty infiltration at nonquantitative MR imaging and with findings at clinical assessment.

### Advances in Knowledge

- The gluteus maximus muscle is the most severely affected muscle of the pelvis and thighs in boys with Duchenne muscular dystrophy (DMD).
- The degree of disease involvement of the muscle, which can be objectively determined by using T2 mapping, reflects the disease severity determined by clinical assessments.

### Implication for Patient Care

- Objective evaluation of disease severity can be determined noninvasively with MR imaging by using T2 mapping, and T2 mapping correlates with functional status in children with DMD.

**Published online**
10.1148/radiol.10091547

**Radiology 2010;** 255:899–908

**Abbreviations:**
CFS = clinical functional score
CK = creatine kinase
DMD = Duchenne muscular dystrophy
OR = odds ratio
ROI = region of interest

**Author contributions:**
Guarantor of integrity of entire study, H.K.K.; study concepts/study design or data acquisition or data analysis/interpretation, all authors; manuscript drafting or manuscript revision for important intellectual content, all authors; approval of final version of submitted manuscript, all authors; literature research, H.K.K.; clinical studies, H.K.K., B.W., B.J.D.; statistical analysis, P.S.H., B.J.D.; and manuscript editing, H.K.K., T.L., P.S.H., J.M.R., B.J.D.

Authors stated no financial relationship to disclose.

## Materials and Methods

This prospective study was approved by the institutional review board, and written consent was obtained from all participants' parents or guardians before enrollment. This study was compliant with the Health Insurance Portability and Accountability Act.

Patients with DMD who presented for MR imaging at Cincinnati Children's Hospital Medical Center (Cincinnati, Ohio) were recruited. Thirty-four boys ranging in age from 4 to 17 years (mean age, 8.5 years) were enrolled. All patients had DMD that was confirmed by means of genetic analysis and/or muscle biopsy. All clinical assessments were performed within 3 months of the MR imaging assessments.

### Imaging Assessments

Imaging assessments including nonquantitative MR imaging and T2 mapping were performed from the iliac crest to the mid-thigh by using a 1.5-T imaging system (12× HD Excite; GE Medical Systems, Milwaukee, Wis) with an eight-channel receive-only phased-array cardiac coil (USA Instruments, Aurora, Ohio). No intravenous contrast medium or sedation was used. Because T2 can be affected by exercise or activity (20), patients were requested to restrain from excessive ambulation or exercise. Restrictions included running, hiking, or long-distance walking for 12 hours before the MR imaging evaluations. The total imaging time for both the nonquantitative MR imaging and T2 mapping sequences ranged from 45 to 60 minutes.

*T2 mapping.*—Axial T2 maps without fat saturation were obtained by using a T2-weighted multisection multiecho sequence to quantify the spatial distribution of T2. An echo train length of 11 was used with the following parameters: repetition time msec/echo time msec, 1500/ 9, 18, 27, 36, 45, 54, 63, 72, 81, 90, and 99; matrix, 256 × 160; section thickness, 10 mm; section gap, 20 mm; and field of view, 20–28 cm. The T2 values calculated with this method have been used previously to evaluate articular cartilage and have been shown to be reproducible among institutions and magnets with varying field strengths (21–23). The acquisition time for each T2 map was approximately 3.5 minutes.

*Nonquantitative MR imaging.*—Each nonquantitative MR imaging study included a water-sensitive sequence in the coronal or axial plane; this was either a fat-suppressed fast spin-echo T2-weighted sequence (2500–5000/ 64–85; echo train length, six to eight; matrix, 256 × 192; section thickness, 6–8 mm; section gap, 1 mm) or a fast spin-echo inversion recovery–weighted sequence (repetition time msec/echo time msec/inversion time msec, 4500/ 35/155; echo train length, eight; matrix, 256 × 192; section thickness, 3–5 mm; section gap, 1–2 mm). Axial and coronal conventional T1-weighted images were obtained without fat suppression (500–600/14–23; matrix, 256 × 192; section thickness, 6–8 mm; section gap, 1 mm). The field of view ranged from 20 to 28 cm and was determined by the patient's size to fully include the gluteal muscles.

### Image Interpretation

*T2 mapping.*—T2 maps were calculated on a pixel-by-pixel basis for the muscles in the transverse plane by using a linear least-squares curve-fitting algorithm. Data were analyzed sequentially by one author (H.K.K.) by using the Cincinnati Children's Hospital Imaging Processing Software written in a programming language (Interactive Data Language; ISS, Boulder, Colo). Signal intensity as a function of echo time was fit to a monoexponential function for each pixel. Axial T2 maps from the pelvic girdle to the mid thigh were generated from the slope of the best fit. The T2 map was color coded pixel by pixel with colors corresponding to a range of T2 values (Fig 1, *A*). For the placement of the region of interest (ROI), three section levels were chosen because they contained the largest area of visible muscle with good differentiation of the different muscle compartments. These three sections (at the level of the sciatic foramen, the greater trochanter-ischial tuberosity, and the very proximal portion of the femoral diaphysis) were selected in each patient (Fig 1, *B*). Eighteen muscles in the right side of the pelvic girdle and right thigh were evaluated. The ROI was obtained by the primary author (H.K.K.) by manually tracing the outline of the individual muscle. The size of the ROI was determined by using the individual muscle size on the axial images. Placement of the ROI of each pelvic and thigh muscle on the T2 map generated a mean T2 and histogram of T2 distribution for each muscle (Fig 1, *C*).

Because a given patient can have different muscle volumes for each muscle, the histogram was normalized according to each ROI.

*Nonquantitative MR imaging.*—To minimize learning bias, patient data were removed from the images. Nonquantitative MR images were presented sequentially and interpreted by two radiologists (T.L., with pediatric radiology fellowship training and 18 years of experience, and H.K.K., with pediatric and musculoskeletal radiology fellowship training and 3 years of experience) in consensus. To minimize memory bias, the time between T2 mapping and nonquantitative MR imaging interpretation was at least 3 months. The muscle with the highest T2 in each patient was then identified on nonquantitative MR images. When the radiologists reviewed the images, they did not know the numeric value of the mean T2.

With use of the axial T1-weighted images, fatty infiltration of the pelvic and thigh musculature was subjectively graded by using a modified version of the scale described by Mercuri et al (24), as follows: grade 0, homogeneous muscle signal intensity without fatty infiltration; grade 1 (minimal), predominantly homogeneous muscle signal intensity with minimal scattered fatty infiltration (often seen in gluteus maximus muscles); grade 2 (mild), mild fatty infiltration with additional patchy areas of intramuscular high T1 signal intensity involving less than 30% of the muscle bulk; grade 3 (moderate), moderate fatty infiltration involving 30%–60% of the muscle bulk, but with preserved

Radiology

**Figure 1**

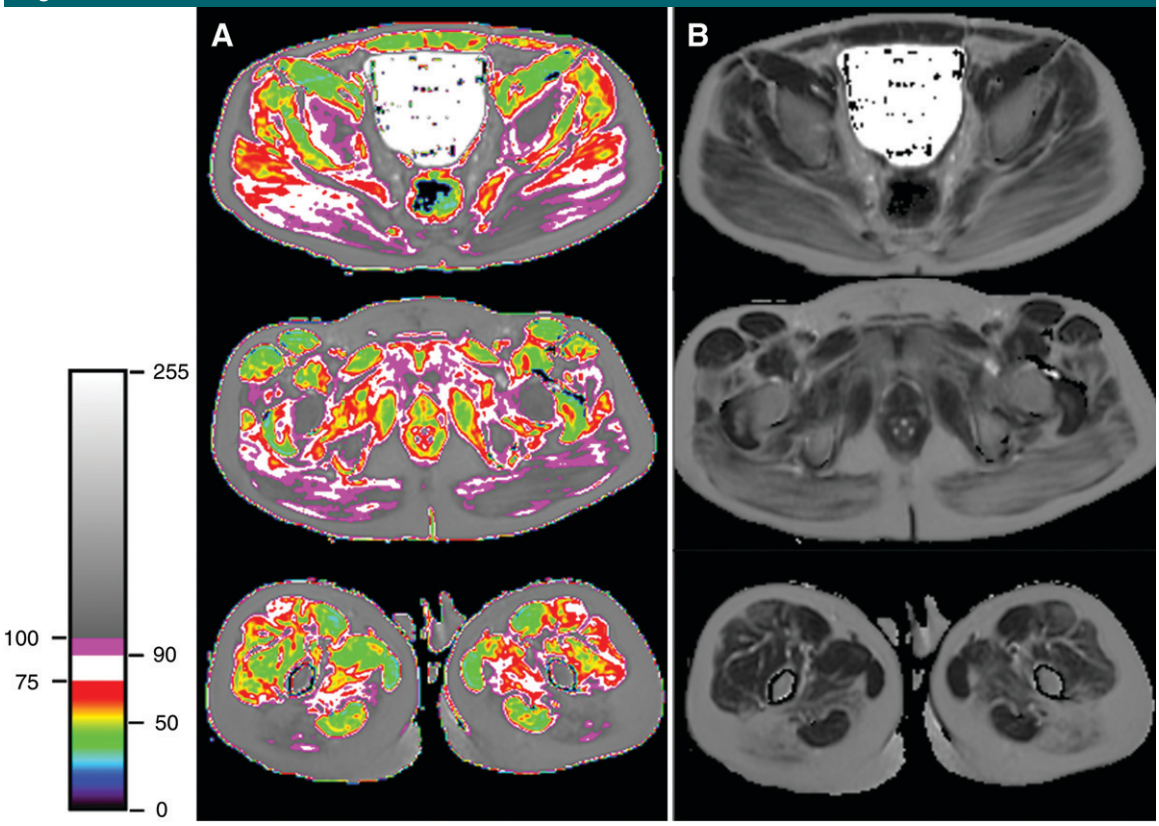


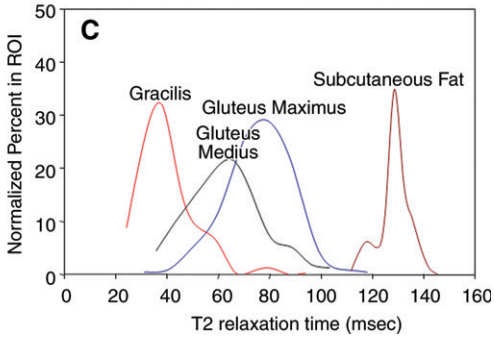


**Figure 1:** Images in an 8-year-old boy with DMD. *A,* Color-coded axial T2 maps (in milliseconds) used to identify the muscles with the highest and lowest T2. *B,* Gray-scale axial T2 maps used for placement of the ROI. Eighteen muscles were identified on three sections (from top to bottom: at the level of sciatic foramen, the greater trochanter-ischial tuberosity, and the very proximal portion of the femoral diaphysis). *C,* Histogram of T2 for three muscles in thigh, pelvis, and subcutaneous fat.

differentiation between muscle and subcutaneous fat; and grade 4 (severe), severe fatty infiltration involving more than 60% of the muscle bulk with loss of demarcation between muscle and subcutaneous fat (Fig 2).

On fast spin-echo inversion-recovery images, the signal intensity of normal muscle is higher than the signal intensity on fat-suppressed fast spin-echo T2-weighted images. This normal increased signal intensity can make it difficult to detect subtle inflammation (16,25). Therefore, muscle inflammation was evaluated on both inversion-recovery and fat-suppressed fast spin-echo T2-weighted images and was compared with that on T1-weighted images obtained in the same location. Grading of inflammation on fast spin-echo inversion-recovery and T2-weighted images was limited to areas that did not show fat with the corresponding T1-weighted sequence. Edema was graded on a subjective scale from grades 0 to 3 by using a modified version of the scale used by Carlo et al (26), as follows: grade 0, absence of edema; grade 1, slight interfascicular edema; grade 2, slight inter- and intrafascicular segmental or global edema; and grade 3, moderate inter- and intrafascicular segmental or global edema.

## Clinical Assessments

All enrolled children underwent clinical assessments by a pediatric neurologist (B.W., with pediatric neurology fellowship training and 12 years of experience) who was blinded to the MR imaging findings. The clinical assessments included the patient's age, CFS, timed Gower score (in seconds), time to run

**Figure 2**

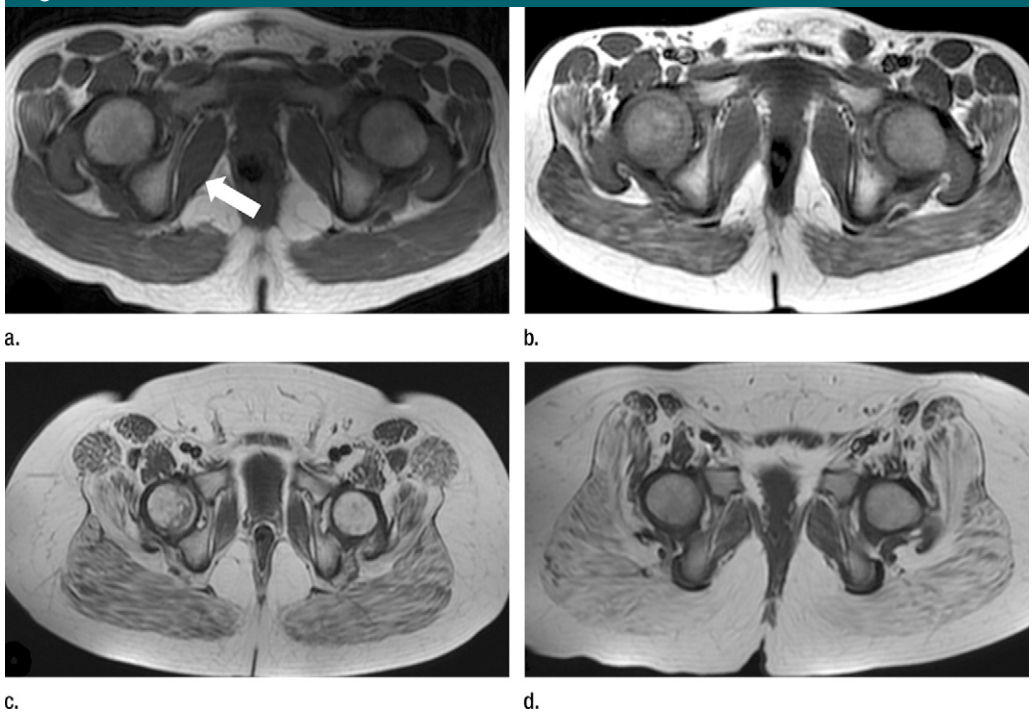


**Figure 2:** Nonquantitative T1-weighted MR images (400–550/14) from four patients show examples of the grading system used to evaluate fatty infiltration of the pelvic muscles. **(a)** No infiltration (grade 0). Homogeneous muscle signal intensity without fatty infiltration, as shown in the right iliacus muscle (arrow), was observed. Grade 1: Predominantly homogeneous muscle signal intensity with minimal scattered fatty infiltration of the gluteus maximus muscle. **(b)** Mild infiltration (grade 2). Mild fatty infiltration with patchy areas of intramuscular high T1 signal intensity involving less than 30% of the muscle bulk was observed. **(c)** Moderate infiltration (grade 3). Moderate fatty infiltration involving 30%–60% of the muscle bulk, but with preserved differentiation between muscle and subcutaneous fat, was observed. **(d)** Severe infiltration (grade 4). Severe fatty infiltration involving more than 60% of the muscle bulk, with loss of demarcation between muscle and subcutaneous fat, was observed.

30 feet (in seconds), and serum CK level. The CFS was assessed by using the Medical Research Council scale with grades 1 (normal) to 8 (severe dysfunction) (10). The timed Gower score was the time the patient needed to rise from a sitting position on the floor to standing. The timed Gower score and time to run 30 feet were only able to be measured in cooperative patients with mild dysfunction (CFS grade 1–3) and were obtained in 30 of 34 patients. Serum CK levels were obtained in 31 patients.

### Statistical Analysis

The Spearman correlation coefficients model was used to evaluate the correlation between mean T2 and nonquantitative MR imaging and clinical assessments (age, CFS, timed Gower score, time to run 30 feet, and serum CK level). Positive and negative correlations were evaluated and considered significant if the *P* value was less than .05. Logistic regression was used to examine the relationship between T2 and the ordinal nonquantitative MR imaging scores for fatty infiltration and inflammation. A two-way analysis of variance was used to look at the T2 responses for the various muscles. The factors were muscle and subject. To adjust for multiple comparisons in this case, a false discovery rate was used with a level of 0.05. All statistical analyses were performed by using statistical software (SAS, version 9.1; SAS Institute, Cary, NC).

## Results

### Disease Distribution on T2 Maps

Overall, the muscle with the longest T2 was the gluteus maximus, with a mean of 79.9 msec ± 19.7 (standard deviation) (Fig 3). The mean T2 of the gluteus maximus muscle was significantly longer than that of the other 17 muscles by using a false discovery rate of 0.05. The shortest T2 was documented in the gracilis muscle, with a mean of 46.94 msec ± 8.7 (Fig 3). The mean T2 of the gracilis muscle was significantly shorter than that of the other 16 muscles, with the exception of the slightly longer T2 of the sartorius muscle. Again, a false discovery rate of .05 was used to determine significance.

### T2 and Nonquantitative MR Imaging

The gluteus maximus muscle showed the greatest cumulative score for fatty infiltration, and the gracilis muscle showed the lowest cumulative score (Fig 4). Grade 4 infiltration was most commonly seen in the gluteus maximus

**Figure 3**

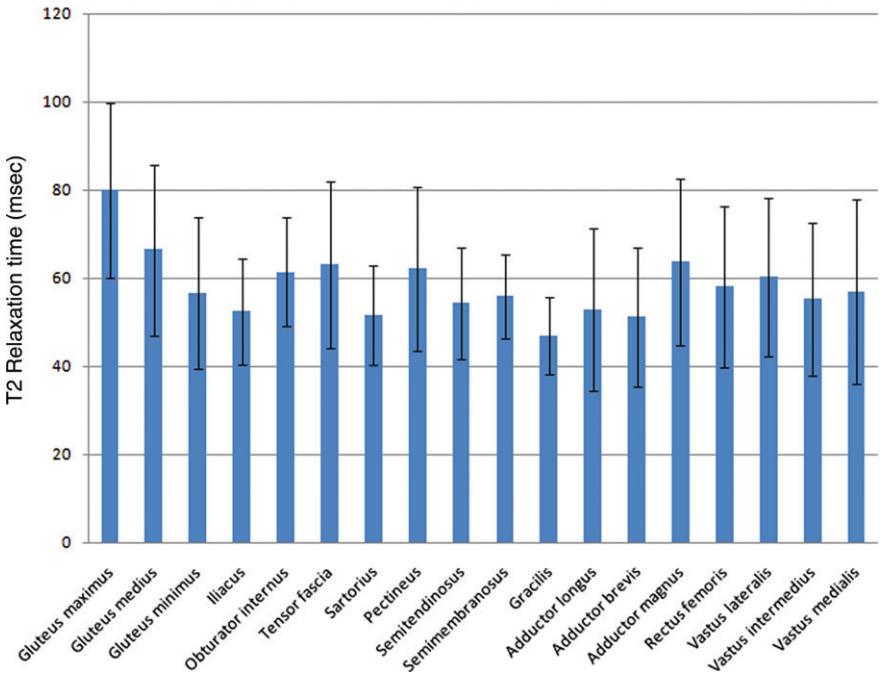


**Figure 3:** Bar chart shows mean T2 (± standard deviation) of 18 pelvic and thigh muscles in 34 patients. The gluteus maximus muscle has the highest mean T2 and the gracilis muscle has the lowest.

**Figure 4**

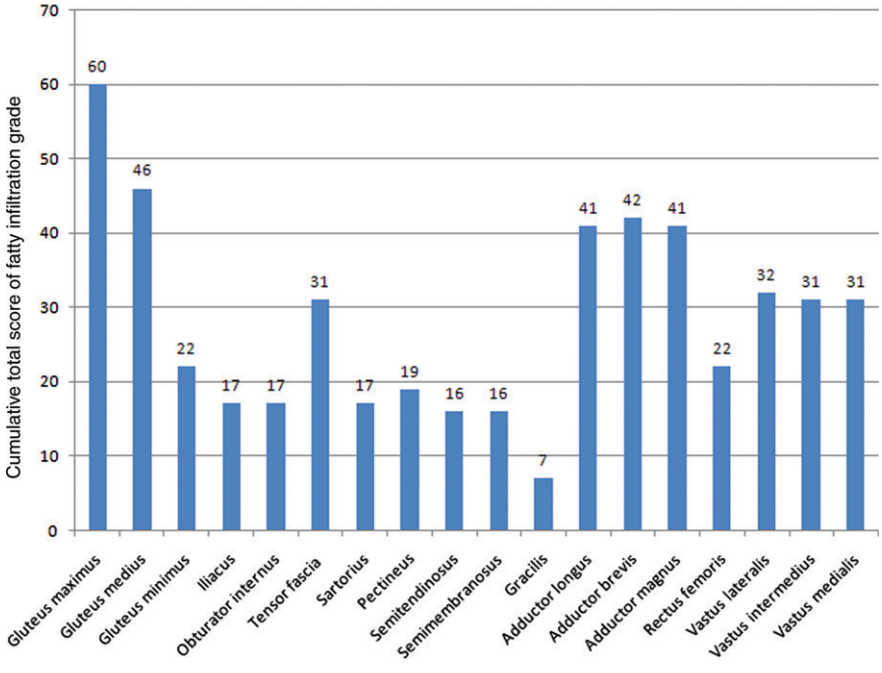


**Figure 4:** Bar chart shows the cumulative total score of all grades of fatty infiltration for each pelvic and thigh muscle on T1-weighted images. The greatest score was seen in the gluteus maximus muscle, and the lowest score was seen in the gracilis muscle.

muscle, whereas grade 0 infiltration was most commonly seen in the gracilis muscle (Fig 5). The infiltration grades of the gluteus maximus muscles were as follows: grade 0, no patients; grade 1, 16 patients; grade 2, 12 patients; grade 3, four patients; and grade 4, two patients.

With the water-sensitive sequences, only two patients had high signal intensity, suggestive of inflammation, in the gluteus maximus muscle; in both patients, this finding was classified as grade 1. In the other 32 patients, the grade was 0.

There was a significant odds ratio (OR) for the T2 of the gluteus maximus muscle and the ordinal nonquantitative MR imaging score of fatty infiltration ($P < .001$). The OR was 1.19, meaning that for each 1-msec increase in T2, the OR of being in one category higher in the nonquantitative MR imaging score of fatty infiltration increased by 19% (95% confidence interval for OR: 1.09, 1.30) (Fig 6). There was no significant OR for the T2 of the gluteus maximus muscle and the nonquantitative MR imaging score of inflammation.

### T2 and Clinical Assessments

There was a significant positive correlation between the T2 of the gluteus maximus muscle and the patient's age ($n = 34$ patients) ($P < .05$), CFS (34 patients) ($P < .001$) (Fig 7), timed Gower score (30 patients) ($P < .05$) (Fig 8), and time to run 30 feet (31 patients) ($P < .05$) (Fig 9). There was no statistically significant correlation between the T2 of the gluteus maximus muscle and serum CK level (determined in 31 of 34 patients) ($P = .35$).

There was a significant OR for the T2 of the gluteus maximus muscle and the ordinal CFS ($P < .001$). The OR was 1.11, so that for each 1-msec increase in T2 response the OR of being in one category higher CFS increased by 11% (95% confidence interval for OR: 1.05, 1.17) (Fig 7).

## Discussion

DMD is an X-linked recessive disorder caused by a genetic defect of the X chromosome at Xp21 that results in partial

**Figure 5**

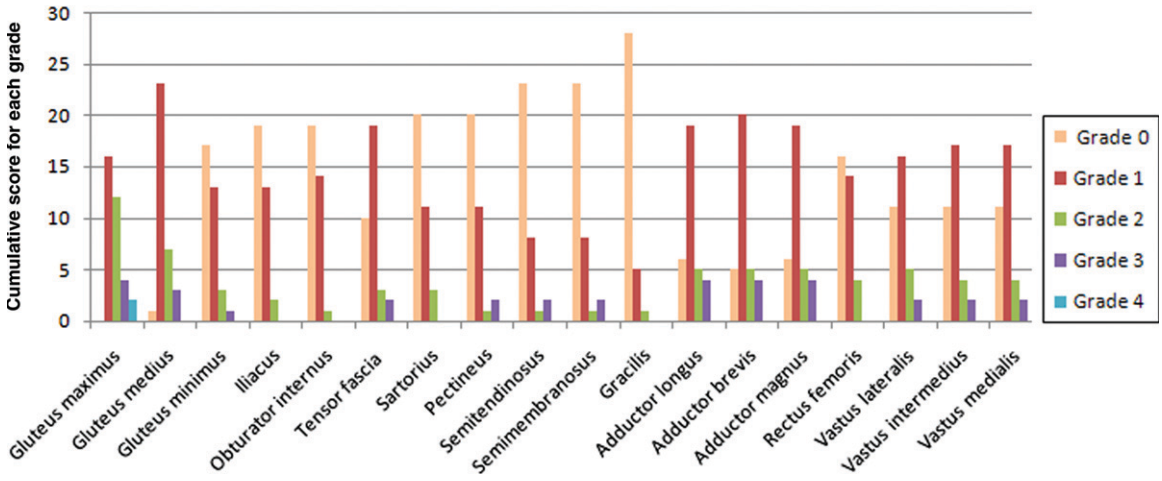


**Figure 5:** Bar chart shows cumulative total score for each grade of fatty infiltration for each pelvic and thigh muscle. Grade 4 infiltration was most commonly seen in the gluteus maximus muscle, and grade 0 infiltration was most commonly seen in the gracilis muscle.

to complete absence of dystrophin (2). Dystrophin-deficient muscles have structural weakness of the sarcolemma and are susceptible to contraction-induced injury (3). Muscle injury is followed by muscle repair and inflammation, which occur early in DMD (4) and ultimately progress to myofibrotic necrosis and replacement of myofibers by fat (27).

DMD has been shown to have a characteristic distribution of fatty infiltration in thigh muscles at nonquantitative MR imaging, with sparing of the gracilis, sartorius, and semitendinosus muscles (15,17). Our results documented the same muscle-sparing pattern with T2 results; the gracilis muscle had the lowest T2, followed by the sartorius muscle.

The T2 of the muscles varies among the different compartments and within each compartment owing to the different water content and the interaction of water with different macromolecules (28). Each motor unit of the muscle has a different T2 because the water content depends on the nonuniform activation in muscle at muscle contraction (20,28,29). Loss of muscle protein and replacement with a different macromolecule such as fat can affect the restricted motion of the water molecule, which contributes to phase dispersion and signal decay. These processes can increase the T2 of muscle water (17,30).

A previous study (18) with a small number of patients with muscular dystrophy showed that T2 mapping of the calf muscles is an objective, quantitative method of differentiating muscle from fat. This same study (18) showed that fatty infiltration within the dystrophic muscle will increase the overall T2. Given these variations of T2, it is important to identify which specific muscle is most consistently involved in the disease process. In our study, the gluteus maximus muscle consistently had the highest T2, and greatest cumulative score for fatty infiltration, and therefore was shown to be the one most consistently involved in the disease and the one that would provide the most accurate indication of disease activity. We suggest that pelvic girdle muscles, especially the gluteus maximus, should be included in MR imaging studies to determine disease severity in DMD.

In our study, there was a significant correlation between T2 and the nonquantitative MR imaging score of fatty infiltration, suggesting that T2 mapping is a quantitative and objective method to measure fatty infiltration within the muscle. Because the grading of fatty infiltration on nonquantitative MR images in DMD is subjective, it can be underestimated or overestimated and can change with the experience of the radiologist and interobserver variance. Conversely, measurement of the T2 of the gluteus maximus muscle is quantitative and objective and can therefore be used during follow-up to assess treatment response, thus avoiding repetitive invasive muscle biopsies. In the future, the mean T2 of the gluteus maximus muscle could be evaluated in a larger number of patients with DMD to establish a means for providing an early diagnosis of DMD.

A previous study in which nonquantitative MR imaging was used for the grading of fatty infiltration showed a positive correlation between the nonquantitative MR imaging score and clinical assessments, including the patient's age and CFS, and a negative correlation between nonquantitative MR imaging score and serum CK level (15). Our study also showed a positive correlation between T2 and clinical assessments, including the patient's age, CFS, timed Gower score, and time to run 30 feet.

The absence of correlation between T2 and serum CK level was not surprising. In patients with DMD, the serum CK level is markedly elevated during the early stages of the disease, and then it decreases with increasing age as muscle producing the serum CK is lost (31). However, the serum CK level can be affected by many other factors; it can be increased by activity (32) and decreased by pharmacologic agents used

**Figure 6**

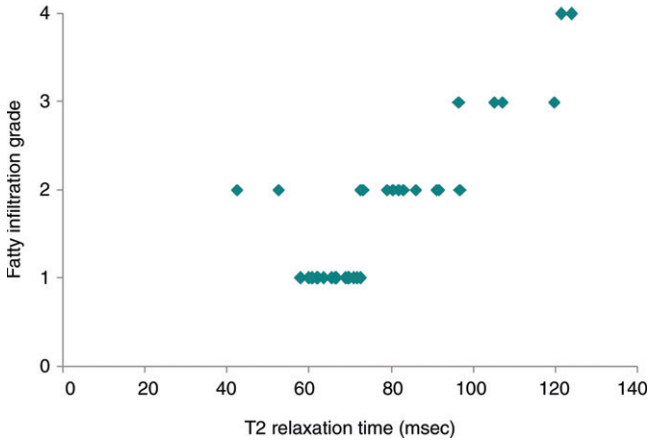


**Figure 6:** Graph shows correlation between T2 and nonquantitative MR imaging score of fatty infiltration in 34 patients. A significant positive correlation was observed between the T2 of the gluteus maximus muscle and the nonquantitative MR imaging score of fatty infiltration ($P < .001$).

**Figure 7**

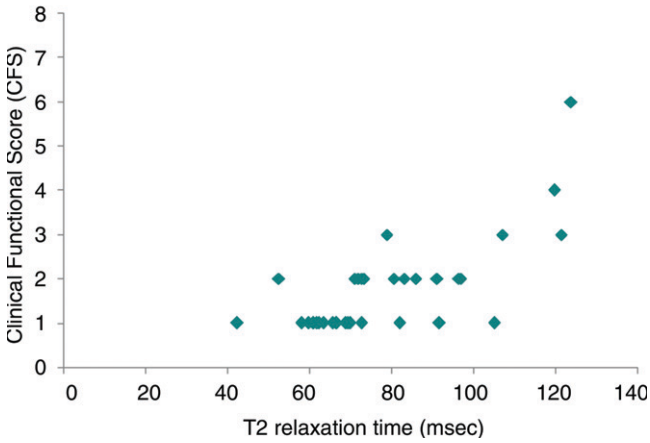


**Figure 7:** Graph shows correlation between T2 and CFS in 34 patients. A significant positive correlation was observed between the T2 of the gluteus maximus muscle and the CFS ($P < .001$).

**Figure 8**

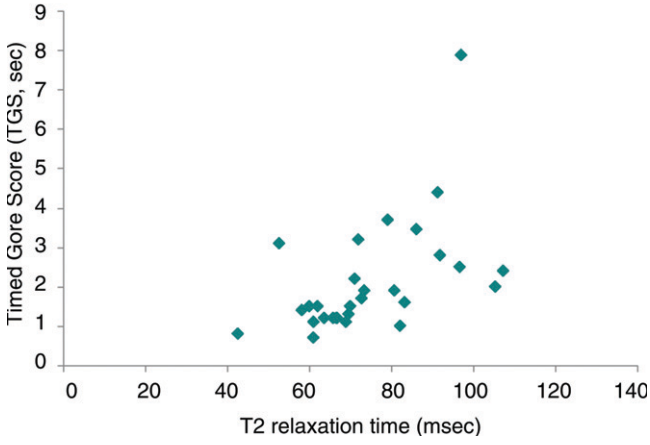


**Figure 8:** Graph shows the correlation between T2 and timed Gower score in 30 patients. A significant positive correlation was observed between the T2 of the gluteus maximus muscle and the timed Gower score ($P < .05$).

**Figure 9**

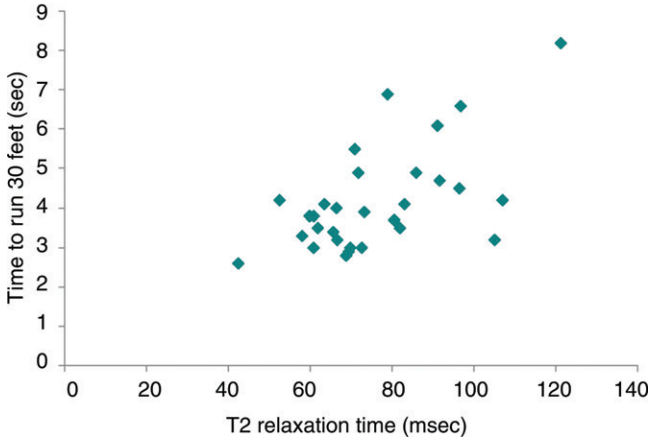


**Figure 9:** Graph shows correlation between T2 and the time to run 30 feet in 30 patients. A significant positive correlation was observed between the T2 of the gluteus maximus muscle and the time to run 30 feet ($P < .05$).

for treating DMD without any change of functional status (33). In our study, the absence of a negative correlation between T2 and serum CK level may be related to those factors and not related to the patient's true functional status.

There were several limitations to this study. T2 can be increased by muscle inflammation (19), which occurs in the earliest stages of DMD. Only two patients in our study showed any subjective inflammation (both grade 1) with the nonquantitative fluid-sensitive MR imaging sequences, and so the effect of edema onT2 is likely to be minimal. Imaging techniques to differentiate between fat and water protons, such as the Dixon technique or iterative decomposition of water and fat with echo asymmetry and least-squares estimation, or IDEAL (34), could be useful in future studies. We used a range of echo times between 9 and 99 msec. These parameters preclude calculation of nonmonoexponential T2 decay (35). Other quantitative studies of T2 have assumed a monoexponential decay, often dictated by stringent parameter limitations of a clinical imaging system (35). Our nonquantitative MR imaging studies were performed without intravenous contrast material. Investigations of contrast material–enhanced MR imaging of skeletal muscle in animal models have shown it to be a sensitive method to detect skeletal muscle damage and inflammation (36,37). We suggest that, in patients with DMD, inflammation on nonquantitative MR images might therefore be underestimated.

T2 can be increased with exercise and muscle activity (20). Although the patients were asked to limit activity before the MR imaging examination, a very small fraction of the mean T2 might have been affected by muscle edema from routine activities (20,38). Fatty infiltration of muscle is the primary disease process in DMD, but it also can be seen in other conditions such as obesity (39,40). We did not control for other possible non-DMD–related fatty infiltration of the muscles.

In conclusion, the gluteus maximus muscle is the most severely affected pelvic girdle muscle in patients with DMD. The T2 of the gluteus maximus muscle can be used as a quantitative measurement of disease involvement and, thus, as an objective measure of disease severity.

## References

1. Danieli GA, Mostacciuolo ML, Bonfante A, Angelini C. Duchenne muscular dystrophy: a population study. Hum Genet 1977;35(2):225–231.
2. Monaco AP. Molecular human genetics and the Duchenne/Becker muscular dystrophy gene. Mol Cell Biol Hum Dis Ser 1993;3:1–11.
3. Petrof BJ, Shrager JB, Stedman HH, Kelly AM, Sweeney HL. Dystrophin protects the sarcolemma from stresses developed during muscle contraction. Proc Natl Acad Sci U S A 1993;90(8):3710–3714.
4. McDouall RM, Dunn MJ, Dubowitz V. Nature of the mononuclear infiltrate and the mechanism of muscle damage in juvenile dermatomyositis and Duchenne muscular dystrophy. J Neurol Sci 1990;99(2-3):199–217.
5. Strober JB. Therapeutics in Duchenne muscular dystrophy. NeuroRx 2006;3(2):225–234.
6. Angelini C. The role of corticosteroids in muscular dystrophy: a critical appraisal. Muscle Nerve 2007;36(4):424–435.
7. Gregorevic P, Chamberlain JS. Gene therapy for muscular dystrophy: a review of promising progress. Expert Opin Biol Ther 2003;3(5):803–814.
8. Skuk D, Goulet M, Roy B, Tremblay JP. Myoblast transplantation in whole muscle of nonhuman primates. J Neuropathol Exp Neurol 2000;59(3):197–206.
9. Law PK, Goodwin TG, Fang Q, et al. Feasibility, safety, and efficacy of myoblast transfer therapy on Duchenne muscular dystrophy boys. Cell Transplant 1992;1(2-3):235–244.
10. Swinyard CA, Deaver GG, Greenspan L. Gradients of functional ability of importance in rehabilitation of patients with progressive muscular and neuromuscular diseases. Arch Phys Med Rehabil 1957;38(9):574–579.
11. Sookhoo S, Mackinnon I, Bushby K, Chinnery PF, Birchall D. MRI for the demonstration of subclinical muscle involvement in muscular dystrophy. Clin Radiol 2007;62(2):160–165.
12. Wren TA, Bluml S, Tseng-Ong L, Gilsanz V. Three-point technique of fat quantification of muscle tissue as a marker of disease progression in Duchenne muscular dystrophy: preliminary study. AJR Am J Roentgenol 2008;190(1):W8–W12.
13. Stern LM, Caudrey DJ, Perrett LV, Boldt DW. Progression of muscular dystrophy assessed by computed tomography. Dev Med Child Neurol 1984;26(5):569–573.
14. Schreiber A, Smith WL, Ionasescu V, et al. Magnetic resonance imaging of children with Duchenne muscular dystrophy. Pediatr Radiol 1987;17(6):495–497.
15. Liu GC, Jong YJ, Chiang CH, Jaw TS. Duchenne muscular dystrophy: MR grading system with functional correlation. Radiology 1993;186(2):475–480.
16. Marden FA, Connolly AM, Siegel MJ, Rubin DA. Compositional analysis of muscle in boys with Duchenne muscular dystrophy using MR imaging. Skeletal Radiol 2005;34(3):140–148.
17. Huang Y, Majumdar S, Genant HK, et al. Quantitative MR relaxometry study of muscle composition and function in Duchenne muscular dystrophy. J Magn Reson Imaging 1994;4(1):59–64.
18. Phoenix J, Betal D, Roberts N, Helliwell TR, Edwards RH. Objective quantification of muscle and fat in human dystrophic muscle by magnetic resonance image analysis. Muscle Nerve 1996;19(3):302–310.
19. Maillard SM, Jones R, Owens C, et al. Quantitative assessment of MRI T2 relaxation time of thigh muscles in juvenile dermatomyositis. Rheumatology (Oxford) 2004;43(5):603–608.
20. Patten C, Meyer RA, Fleckenstein JL. T2 mapping of muscle. Semin Musculoskelet Radiol 2003;7(4):297–305.
21. Kight AC, Dardzinski BJ, Laor T, Graham TB. Magnetic resonance imaging evaluation of the effects of juvenile rheumatoid arthritis on distal femoral weight-bearing cartilage. Arthritis Rheum 2004;50(3):901–905.
22. Dardzinski BJ, Laor T, Schmithorst VJ, Klosterman L, Graham TB. Mapping T2 relaxation time in the pediatric knee: feasibility with a clinical 1.5-T MR imaging system. Radiology 2002;225(1):233–239.
23. Dardzinski BJ, Mosher TJ, Li S, Van Slyke MA, Smith MB. Spatial variation of T2 in human articular cartilage. Radiology 1997;205(2):546–550.
24. Mercuri E, Pichiecchio A, Allsop J, Messina S, Pane M, Muntoni F. Muscle MRI in inherited neuromuscular disorders: past, present, and future. J Magn Reson Imaging 2007;25(2):433–440.
25. Jaramillo D, Laor T. Pediatric musculoskeletal MRI: basic principles to optimize success. Pediatr Radiol 2008;38(4):379–391.
26. Carlo B, Roberta P, Roberto S, Marina F, Corrado A. Limb-girdle muscular dystrophies type 2A and 2B: clinical and radiological aspects. Basic Appl Myol 2006;16(1):17–25.
27. Kliegman R, Nelson WE. Nelson textbook of pediatrics. Philadelphia, Pa: Saunders, 2007.
28. Prior BM, Foley JM, Jayaraman RC, Meyer RA. Pixel T2 distribution in functional magnetic resonance images of muscle. J Appl Physiol 1999;87(6):2107–2114.
29. Sjøgaard G, Saltin B. Extra- and intracellular water spaces in muscles of man at rest and with dynamic exercise. Am J Physiol 1982;243(3):R271–R280.
30. Fullerton GD, Cameron IL, Hunter K, Fullerton HJ. Proton magnetic resonance relaxation behavior of whole muscle with fatty inclusions. Radiology 1985;155(3):727–730.
31. Zatz M, Rapaport D, Vainzof M, et al. Serum creatine-kinase (CK) and pyruvate-kinase (PK) activities in Duchenne (DMD) as compared with Becker (BMD) muscular dystrophy. J Neurol Sci 1991;102(2):190–196.
32. Malm C, Nyberg P, Engstrom M, et al. Immunological changes in human skeletal muscle and blood after eccentric exercise and multiple biopsies. J Physiol 2000;529(pt 1):243–262.
33. Davies KE. Challenges in Duchenne muscular dystrophy. Neuromuscul Disord 1997;7(8):482–486.
34. Costa DN, Pedrosa I, McKenzie C, Reeder SB, Rofsky NM. Body MRI using IDEAL. AJR Am J Roentgenol 2008;190(4):1076–1084.

35. Ababneh Z, Beloeil H, Berde CB, Gambarota G, Maier SE, Mulkern RV. Biexponential parameterization of diffusion and T2 relaxation decay curves in a rat muscle edema model: decay curve components and water compartments. Magn Reson Med 2005;54(3):524–531.

36. Straub V, Donahue KM, Allamand V, Davisson RL, Kim YR, Campbell KP. Contrast agent–enhanced magnetic resonance imaging of skeletal muscle damage in animal models of muscular dystrophy. Magn Reson Med 2000;44(4):655–659.

37. Schmidt S, Vieweger A, Obst M, et al. Dysferlin-deficient muscular dystrophy: gadofluorine M suitability at MR imaging in a mouse model. Radiology 2009;250(1):87–94.

38. Ploutz-Snyder LL, Nyren S, Cooper TG, Potchen EJ, Meyer RA. Different effects of exercise and edema on T2 relaxation in skeletal muscle. Magn Reson Med 1997;37(5):676–682.

39. Goodpaster BH, Thaete FL, Kelley DE. Composition of skeletal muscle evaluated with computed tomography. Ann N Y Acad Sci 2000;904:18–24.

40. Goodpaster BH, Stenger VA, Boada F, et al. Skeletal muscle lipid concentration quantified by magnetic resonance imaging. Am J Clin Nutr 2004;79(5):748–754.